

Advanced oxidation protein products induce apoptosis, and upregulate sclerostin and RANKL expression, in osteocytic MLO-Y4 cells via JNK/p38 MAPK activation

CHAOQUN YU¹, DONG HUANG¹, KUNYUAN WANG², BOCHUAN LIN¹,
YUANHANG LIU¹, SONGBO LIU¹, WEICHI WU¹ and HUIRU ZHANG¹

¹Department of Traumatology and Microsurgery, The Third Clinical College, Southern Medical University, Guangdong No. 2 Provincial People's Hospital; ²Department of Nephrology, The First Clinical College, Southern Medical University, Guangzhou, Guangdong 510310, P.R. China

Received September 21, 2015; Accepted August 31, 2016

DOI: 10.3892/mmr.2016.6047

Abstract. Advanced oxidation protein products (AOPPs) are recognized as novel markers of oxidative stress and contribute to various medical conditions, which are associated with secondary osteoporosis. However, little is currently known regarding the role of AOPPs in the development of secondary osteoporosis. As the commander cells of bone remodeling, osteocytes are involved in the pathogenesis of osteoporosis. The present study aimed to determine the cytotoxic mechanisms of AOPPs on osteocytic MLO-Y4 cells. The results demonstrated that treatment with AOPPs significantly triggered apoptosis of MLO-Y4 cells, in a dose- and time-dependent manner. Furthermore, exposure to AOPPs induced phosphorylation of c-Jun N-terminal kinases (JNK) and p38 mitogen-activated protein kinases (MAPK). Conversely, N-acetylcysteine inhibited the activation of JNK and p38 MAPK, thus suggesting that the AOPPs-induced activation of JNK/p38 MAPK is reactive oxygen species (ROS)-dependent. In addition, SB203580 and SP600125 suppressed apoptosis, but did not affect ROS production, following AOPPs treatment. Notably, AOPPs also induced a significant upregulation in the expression levels of sclerostin and receptor activator of nuclear factor kappa-B ligand (RANKL) in a JNK/p38 MAPK-dependent manner. These findings provide novel insights into the molecular mechanisms underlying AOPPs-mediated cell death, and suggest that modulation of apoptotic pathways via the MAPK

signaling cascade may be considered a therapeutic strategy for the prevention and treatment of secondary osteoporosis.

Introduction

Advanced oxidation protein products (AOPPs) were initially described by Witko-Sarsat *et al* in 1996 as a family of oxidized, dityrosine-containing protein products, which are formed during oxidative stress by the interaction between plasma proteins and chlorinated oxidants, and are often carried by albumin *in vivo* (1,2). AOPPs are recognized as novel markers of protein oxidative damage, the intensity of oxidative stress, and inflammation (3). Significantly increased concentrations of AOPPs have been detected in several pathological conditions, including chronic kidney disease, diabetes mellitus, inflammatory bowel disease and rheumatoid arthritis (4-6).

Notably, patients with the aforementioned conditions often exhibit bone loss and have an increased incidence of fracture, which is defined as secondary osteoporosis. Secondary osteoporosis is characterized by low bone mass with micro-architectural alterations in the bone, which can lead to fragility fractures in the presence of an underlying disease or medication (7). The exact underlying mechanisms of this condition remain unclear; however, it may be hypothesized that AOPPs have a certain role in the progression of secondary osteoporosis.

In the process of bone remodeling, bone is constantly renewed by the balance between osteoblastic bone formation and osteoclastic bone resorption. Previous studies have demonstrated that AOPPs may inhibit the proliferation and differentiation of rat osteoblastic cells and rat mesenchymal stem cells (8,9). As the most abundant cell type in bone (90-95%), osteocytes function as more than just mechanosensors in bone homeostasis. It has previously been reported that osteocytes are a major source of the cytokine receptor activator of nuclear factor kappa-B ligand (RANKL), which is a ligand for osteoprotegerin and functions as a key factor for osteoclast differentiation and activation (10,11). In addition, osteocytes almost exclusively secrete the protein sclerostin, which inhibits osteoblast functioning and bone formation by

Correspondence to: Professor Dong Huang, Department of Traumatology and Microsurgery, The Third Clinical College, Southern Medical University, Guangdong No. 2 Provincial People's Hospital, 1 Shiliugang Road, Haizhu, Guangzhou, Guangdong 510310, P.R. China
E-mail: huangdong_gd2h@163.com

Key words: advanced oxidation protein products, osteocyte, sclerostin, RANKL, apoptosis, mitogen-activated protein kinases, reactive oxygen species

antagonizing the Wnt signaling pathway (12,13). Therefore, it has been suggested that osteocytes act as the commander cells of bone remodeling, since they regulate bone formation and bone resorption via sclerostin and RANKL. However, it remains unclear whether AOPPs affect osteocytes or regulate the production of these factors, thereby causing bone deterioration in patients with pathological levels of plasma AOPPs.

Oxidative stress induces several signal transduction pathways, including the mitogen-activated protein kinases (MAPKs) pathways. MAPKs consist of extracellular signal-regulated kinases (ERK), c-Jun N-terminal kinases (JNK) and p38 MAPK, and mediate various cellular activities, including cell growth, differentiation, survival and death (14,15). It has previously been reported that JNK/p38 MAPK pathways have a pivotal role in oxidative stress-induced apoptosis, whereas ERK exerts effects on cell physiology. However, it remains unknown as to whether AOPPs activate JNK/p38 MAPK signaling in osteocytes, or whether these signaling pathways are essential for AOPPs-induced apoptosis.

The present study aimed to determine the effects of AOPPs on apoptosis and on the expression of sclerostin and RANKL in osteocytic MLO-Y4 cells. The results demonstrated that AOPPs induced apoptosis of MLO-Y4 cells, and increased sclerostin and RANKL expression in a dose- and time-dependent manner. In addition, the association between JNK/p38 MAPK signaling and AOPPs-induced apoptosis was investigated, and it was revealed that sustained activation of the JNK/p38 MAPK pathways is responsible for AOPPs-induced apoptosis of osteocytic MLO-Y4 cells.

Materials and methods

Reagents. Mouse serum albumin (MSA), p38 inhibitor SB203580, JNK inhibitor SP600125, ERK inhibitor PD98059, N-acetylcysteine (NAC) and apocynin were obtained from Sigma-Aldrich (Merck Millipore, Darmstadt, Germany). Trypsin-EDTA, fetal bovine serum (FBS), newborn calf serum, α -minimum essential medium (α -MEM) and penicillin-streptomycin were purchased from Gibco (Thermo Fisher Scientific, Inc., Waltham, MA, USA). TRIzol[®] reagent was obtained from Invitrogen (Thermo Fisher Scientific, Inc.). The Prime Script[®] One Step real time-polymerase chain reaction (RT-PCR) kit and SYBR *Premix Ex Taq* were obtained from Takara Biotechnology Co., Ltd. (Dalian, China). Radioimmunoprecipitation assay (RIPA) lysis buffer and phenylmethylsulfonyl fluoride (PMSF) were from Beyotime Institute of Biotechnology (Shanghai, China). The Detoxi-Gel column was from Pierce (Thermo Fisher Scientific, Inc.). Cell Death Detection enzyme-linked immunosorbent assay (ELISA)^{PLUS} kit and Annexin V-fluorescein isothiocyanate (FITC) Apoptosis Detection kit were obtained from Roche Life Science (Indianapolis, IN, USA). Rabbit anti-sclerostin (cat. no. sc-130258) and anti-RANKL (cat. no. sc-9073) antibodies were from Santa Cruz Biotechnology, Inc. (Dallas, TX, USA); anti-phosphorylated (P)-p38 (cat. no. #4631S), anti-p38 (cat. no. #9212S), anti-P-ERK 1/2 (cat. no. #9101S), anti-ERK 1/2 (cat. no. #9102S), anti-P-JNK (cat. no. #9251S) and anti-JNK (cat. no. #9252S) antibodies were from Cell Signaling Technology, Inc. (Beverly, MA, USA). Mouse anti-glyceraldehyde 3-phosphate dehydrogenase (GAPDH)

(cat. no. ab8245) antibody and the Cellular Reactive Species Detection Assay kit were purchased from Abcam (Cambridge, UK).

AOPPs-MSA preparation and determination. AOPPs-MSA was prepared *in vitro* by incubating 20 mg/ml MSA with 200 mM hypochlorous acid (HOCl) for 30 min at 37°C. The mixture was then dialyzed overnight against phosphate-buffered saline to remove any free HOCl. All prepared samples were passed through a Detoxi-Gel column to remove contaminated endotoxin. Endotoxin levels in the preparation were determined using the Limulus Amebocyte Lysate kit (Sigma-Aldrich; Merck Millipore) and were shown to be <0.025 EU/ml. AOPP content in the preparation was determined according to a previously published method (1). Briefly, 200 μ l of the sample or chloramine-T (standard curve; Sigma-Aldrich; Merck Millipore) were plated in a 96-well plate and mixed with 20 μ l acetic acid. The absorbance was read immediately at 340 nm using a microplate reader (Multiskan MK3; Thermo Fisher Scientific, Inc.). The content of AOPP in the AOPP-MSA preparation was 68.80 \pm 5.35 nmol/mg protein in AOPPs-MSA, and 0.27 \pm 0.03 nmol/mg protein in native MSA.

Cell culture. Mouse osteocyte-like MLO-Y4 cells were kindly provided by Dr. Ni Guoxin (Southern Medical University, Guangzhou, China). The cells were cultured on type I collagen-coated plates in α -MEM at 37°C in a humidified atmosphere containing 5% CO₂. The medium was supplemented with 5% newborn calf serum (CS), 5% FBS and 1% penicillin-streptomycin.

Protein extraction and western blot analysis. Cells were lysed with RIPA buffer containing 0.5 mM PMSF, and the lysates were centrifuged prior to determination of the protein concentration using a bicinchoninic acid kit (Sigma-Aldrich; Merck Millipore). A total of 30 μ g of protein was loaded per sample channel, and the proteins were separated by sodium dodecyl sulfate-polyacrylamide gel electrophoresis (8% gels). The separated proteins were then transferred to polyvinylidene fluoride membranes. The membranes were blocked with blocking buffer (5% defatted milk) and incubated at room temperature for 1 h. The membranes were initially probed with anti-sclerostin (1:500 dilution), anti-RANKL (1:500 dilution), anti-P-p38, anti-P-ERK 1/2 and anti-P-JNK (all 1:1,000 dilution) primary antibodies, and incubated at 4°C overnight. Subsequently, membranes were stripped and reprobed with anti-ERK 1/2, anti-JNK, anti-p38 (all 1:1,000 dilution) or anti-GAPDH (1:500 dilution) for normalization and densitometric analysis. Blots were scanned and visualized using the Odyssey detector, as mentioned below. After extensive washing with Tris-buffered saline/Tween 20 (TBS-T), the membranes were incubated for 1 h at room temperature with the secondary antibody [IRDye[®] 680LT-conjugated donkey anti-rabbit immunoglobulin G (IgG) (H + L) antibody; cat. no. P/N 925-68023, 1:20,000 dilution). Images were detected using the Odyssey detector (LI-COR Biosciences, Lincoln, NE, USA).

RNA extraction and reverse transcription-quantitative (RT-qPCR). Total RNA was extracted from the lysed cells using TRIzol[®] reagent. Aliquots of each RNA extraction

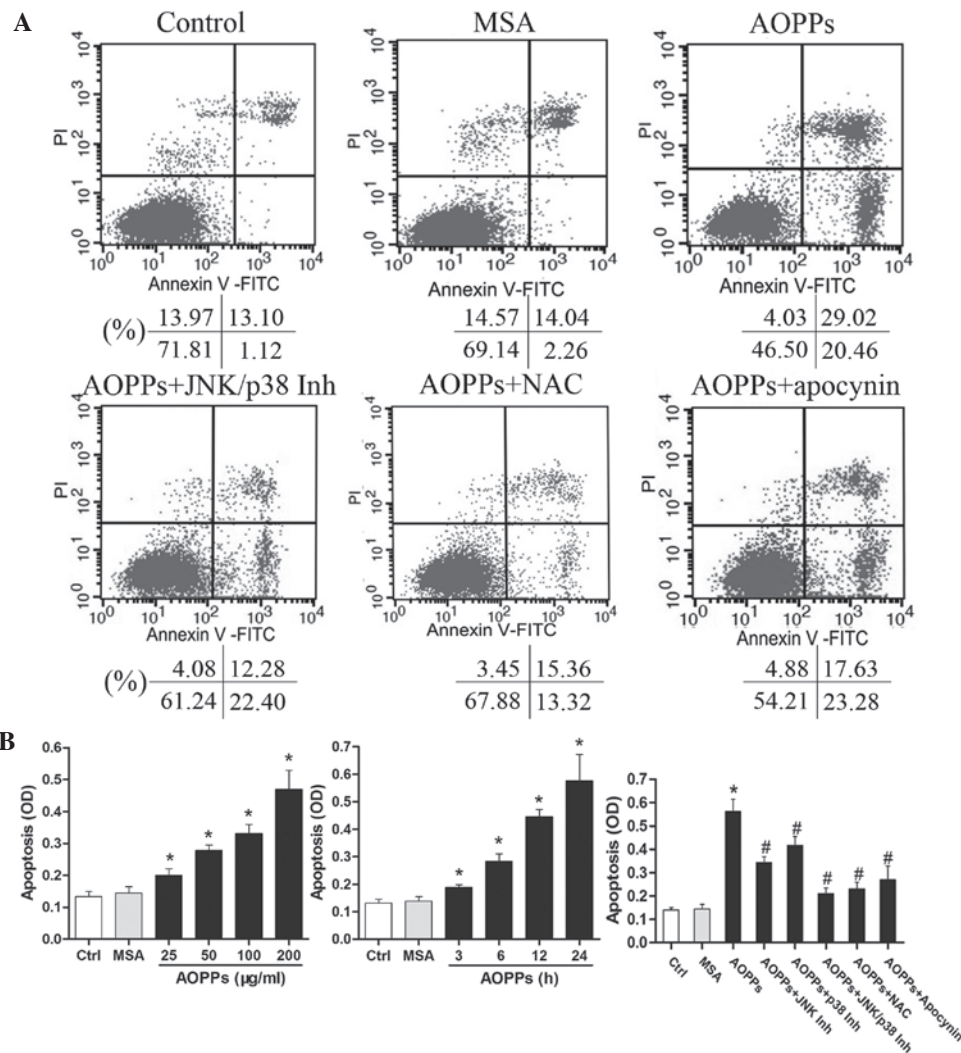


Figure 1. Treatment with advanced oxidation protein products (AOPPs) significantly induced apoptosis of cultured MLO-Y4 cells. (A) Serum-starved MLO-Y4 cells were pretreated with c-Jun N-terminal kinases (JNK) inhibitor SP600125 (30 μ M), p38 inhibitor SB203580 (30 μ M), reactive oxygen species (ROS) scavenger N-acetylcysteine (NAC) (10 μ M) and NADPH oxidase inhibitor apocynin (100 μ M), prior to incubation with 200 μ g/ml AOPPs-mouse serum albumin (MSA) for 24 h. The percentage of apoptotic cells was estimated by Annexin V/propidium iodide (PI) staining. Dot plot graphs present the percentage of viable cells, early-phase apoptotic cells, late-phase apoptotic cells and necrotic cells. (B) Apoptotic cells were also detected using the Cell Death Detection enzyme-linked immunosorbent assay (ELISA) kit. MLO-Y4 cells were incubated with the indicated concentrations of AOPPs for 24 h, or with 200 μ g/ml AOPPs for the indicated durations, and were subjected to ELISA assay. AOPPs induced apoptosis of MLO-Y4 cells in a dose- and time-dependent manner. To verify the effects of JNK/p38-mitogen-activated protein kinases signaling, ROS and NADPH oxidase on AOPPs-induced apoptosis, the experiments were repeated in the presence of SP600125, SB203580, NAC and apocynin. Data are presented as the mean \pm standard deviation of three independent experiments. Analysis of variance; *P<0.05 vs. control; #P<0.05 vs. AOPPs-treated group. Ctrl, untreated cells; AOPPs, AOPPs-MSA; FITC, fluorescein isothiocyanate; Inh, inhibitor; OD, optical density.

were then reverse transcribed simultaneously into cDNA using the PrimeScript[®] One Step RT-PCR kit, according to the manufacturer's protocol. RT-qPCR was performed in a total volume of 20 μ l in duplicate using the SYBR[®] Premix Ex Taq kit and Fast Real-time PCR system 7300 (Applied Biosystems; Thermo Fisher Scientific, Inc.). The PCR reaction mixture contained 2X SYBR[®] Premix Ex Taq[™] (10 μ l), PCR forward primer (10 μ M; 0.4 μ l), PCR reverse primer (10 μ M; 0.4 μ l), ROX Reference Dye II (50x; 0.4 μ l), RT reaction solution (cDNA) (2.0 μ l) and double-distilled H₂O (6.8 μ l). The PCR thermocycling conditions were as follows: Stage 1: 95°C for 30 sec, repeat one time; Stage 2: 95°C for 5 sec, 60°C for 34 sec, repeat 40 times; Stage 3: 95°C for 15 sec, 60°C for 60 sec and 95°C for 15 sec, repeat one time. The mRNA value for each gene was normalized relative to the mouse GAPDH

mRNA levels in the same RNA samples, and the results were quantified using the 2^{- $\Delta\Delta$ CT} method (16). Primer sequences were as follows: GAPDH, forward 5'-ATGGCCTTCCGTGTT CCTAC-3', reverse 5'-CACCTTCTTGATGTCATCATACTT G-3'; sclerostin (gene name, SOST), forward 5'-GCCTCCTCA GGAAGTAGAGAAC-3', reverse 5'-TACTCGGACACGTCT TTGGTG-3'; and RANKL, forward 5'-TGTACTTTTCGAG CGCATGATG-3' and reverse 5'-AGGCTTGTTCATCCTCC TG-3'.

Determination of intracellular formation of reactive oxygen species (ROS). Intracellular ROS were detected in MLO-Y4 cells using the Cellular Reactive Species Detection Assay kit (Deep Red Fluorescence). Briefly, ROS assay solution (100 μ l/well) was added to the treated or untreated cells at a

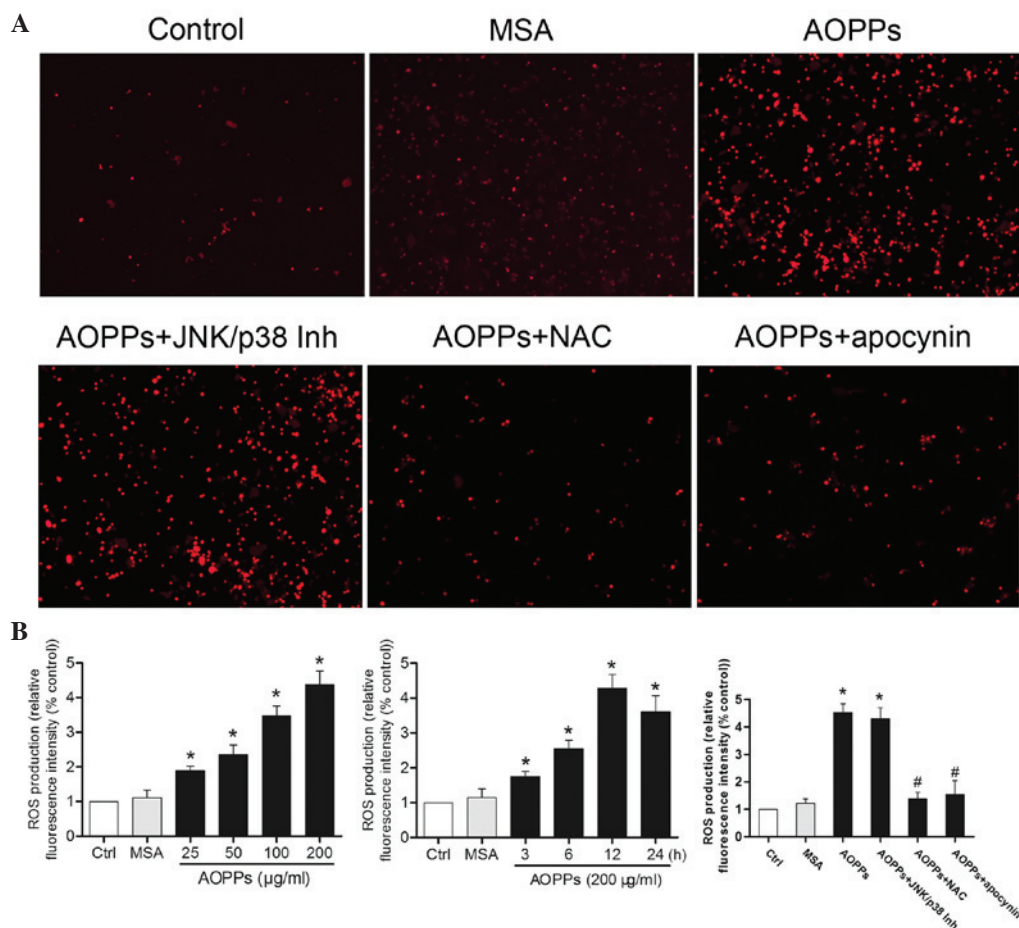


Figure 2. Advanced oxidation protein products (AOPPs) induced reactive oxygen species (ROS) production in MLO-Y4 cells. Serum-starved MLO-Y4 cells were treated with the indicated concentrations of AOPPs for 24 h, or with 200 $\mu\text{g}/\text{ml}$ of AOPPs for the indicated durations. Intracellular ROS production was determined by respectively measuring the fluorescence intensity using the Cellular Reactive Species Detection Assay kit (Deep Red Fluorescence). (A) Representative fluorescence images of AOPPs-induced ROS generation; N-acetylcysteine (NAC) and NADPH oxidase inhibitor apocynin could reduce ROS generation. Magnification, $\times 100$. (B) AOPPs induced overproduction of intracellular ROS in a dose- and time-dependent manner. Data are presented as the mean \pm standard deviation of three independent experiments. Analysis of variance; * $P < 0.05$ vs. control; # $P < 0.05$ vs. AOPPs-treated group. Ctrl, untreated cells; MSA, mouse serum albumin; AOPPs, AOPPs-MSA; Inh, inhibitor.

density of 3,000 cells per well, and the cells were incubated in a 5% CO_2 atmosphere at 37°C in an incubator for 1 h. The fluorescence signal was monitored at an excitation wavelength of 650 nm and an emission wavelength of 675 nm. Untreated cells were used to determine background fluorescence. Data were expressed as percentage of controls.

Measurement of apoptotic cell death. To detect apoptosis, the Cell Death Detection ELISA^{PLUS} kit was used. Briefly, MLO-Y4 cells were seeded in 96-well plates at a density of 3,000 cells/well and were incubated overnight in α -MEM supplemented with 5% FBS and 5% CS at 37°C in a humidified atmosphere containing 5% CO_2 . On the following day, the cells were treated with either MSA (control) or various concentrations of AOPPs for 60 min, or with 200 $\mu\text{g}/\text{ml}$ AOPPs for the indicated time. The cells were then lysed, and the supernatant was analyzed using the Cell Death Detection ELISA^{PLUS} kit, according to the manufacturer's protocol.

Annexin V/propidium iodide (PI) staining assay. Another apoptosis analysis was conducted using the Annexin V/PI assay. The Annexin V-FITC Apoptosis Detection kit was used in

accordance with the manufacturer's protocol. Briefly, MLO-Y4 cells were serum-starved for 24 h, and were pretreated for 30 min at 37°C with JNK inhibitor SP600125 (30 μM), p38 inhibitor SB203580 (30 μM), ROS scavenger NAC (10 μM) and NADPH oxidase inhibitor apocynin (100 μM), prior to incubation with the indicated concentration of AOPPs-MSA for 24 h. Cells were trypsinized and double-stained with FITC-conjugated Annexin V and PI. Cells were analyzed using a flow cytometer (Beckman Coulter, Brea, CA, USA).

Statistical analysis. All experiments were performed in triplicate. Data are presented as the mean \pm standard deviation. One-way analysis of variance was performed, followed by a least significant difference (LSD) method when $P < 0.05$ for multiple comparisons. Statistical analyses were conducted using SPSS 19.0 (IBM SPSS, Armonk, NY, USA). $P < 0.05$ was considered to indicate a statistically significant difference.

Results

AOPPs induce apoptosis of MLO-Y4 cells. The present study initially investigated whether AOPPs induced apoptosis of

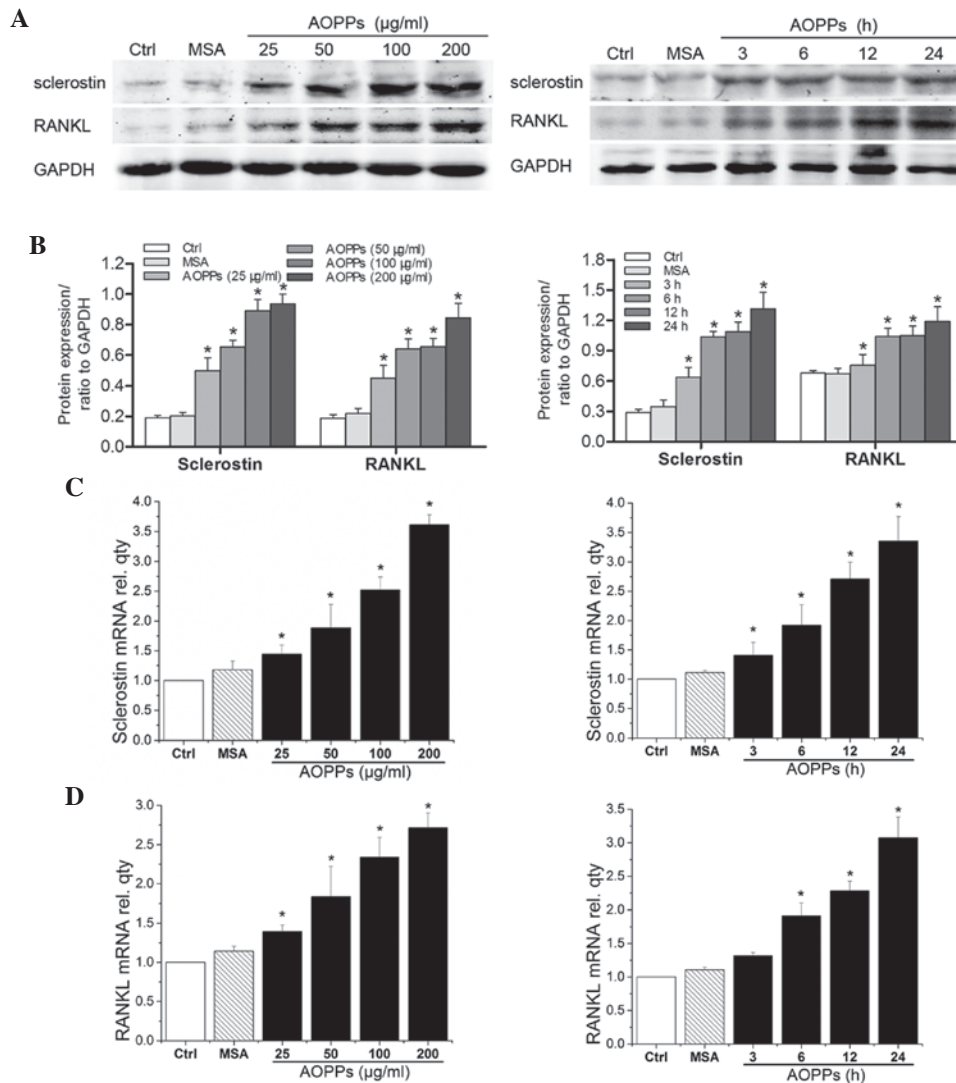


Figure 3. Treatment with advanced oxidation protein products (AOPPs) increased the expression levels of sclerostin and receptor activator of nuclear factor kappa-B ligand (RANKL) in cultured MLO-Y4 cells. MLO-Y4 cells were incubated with the indicated concentrations of AOPPs for 24 h, or with 200 µg/ml AOPPs for the indicated durations, and were subjected to (A and B) protein and (C and D) mRNA analysis of sclerostin and RANKL. Treatment with AOPPs increased the expression levels of (A-C) sclerostin and (A, B and D) RANKL, at the mRNA and protein levels, in a dose- and time-dependent manner. Data are presented as the mean ± standard deviation of three independent experiments. Analysis of variance; *P<0.05 vs. control. Ctrl, control; MSA, mouse serum albumin; AOPPs, AOPPs-MSA; GAPDH, glyceraldehyde 3-phosphate dehydrogenase; rel. qty, relative quantity.

osteocytic MLO-Y4 cells (Fig. 1). As determined by Cell Death Detection ELISA kit and Annexin V/PI staining, treatment of the cells with AOPPs significantly induced apoptosis in a dose- and time-dependent manner (Fig. 1A and B). Subsequently, the present study examined the effects of JNK inhibitor SP600125 (30 µM), p38 inhibitor SB203580 (30 µM), ROS scavenger NAC (10 µM) and NADPH oxidase inhibitor apocynin (100 µM) on AOPPs-induced apoptosis. Pretreatment of the cells with these agents significantly reversed AOPPs-induced apoptosis (Fig. 1B).

AOPPs enhance intracellular ROS generation in MLO-Y4 cells. ROS generation was detected using the Cellular Reactive Species Detection Assay kit (Fig. 2). Treatment of MLO-Y4 cells with AOPPs induced a significant increase in intracellular ROS production, in a dose- and time-dependent manner (Fig. 2B). Conversely, AOPPs-induced ROS generation was suppressed by NAC pretreatment, but not by SP600125 or SB203580

treatment. In addition, the NADPH oxidase inhibitor apocynin exhibited inhibitory action on ROS generation (Fig. 2A and B).

AOPPs increase the expression levels of sclerostin and RANKL in MLO-Y4 cells. Sclerostin and RANKL are associated with bone remodeling by regulating osteoblastogenesis and osteoclastogenesis. Therefore, the present study examined the effects of AOPPs on the expression levels of sclerostin and RANKL in MLO-Y4 cells. As shown in Fig. 3, exposure of MLO-Y4 cells to AOPPs significantly increased the expression of sclerostin, at the protein and mRNA levels (Fig. 3A-C), in a dose- and time-dependent manner. In addition, the effects of AOPPs on the expression levels of RANKL were detected by western blotting and RT-qPCR. Treatment with AOPPs also increased the expression levels of RANKL (Fig. 3A, B and D). However, treatment of the cells with medium alone or MSA did not exert any effects on the expression levels of sclerostin and RANKL.

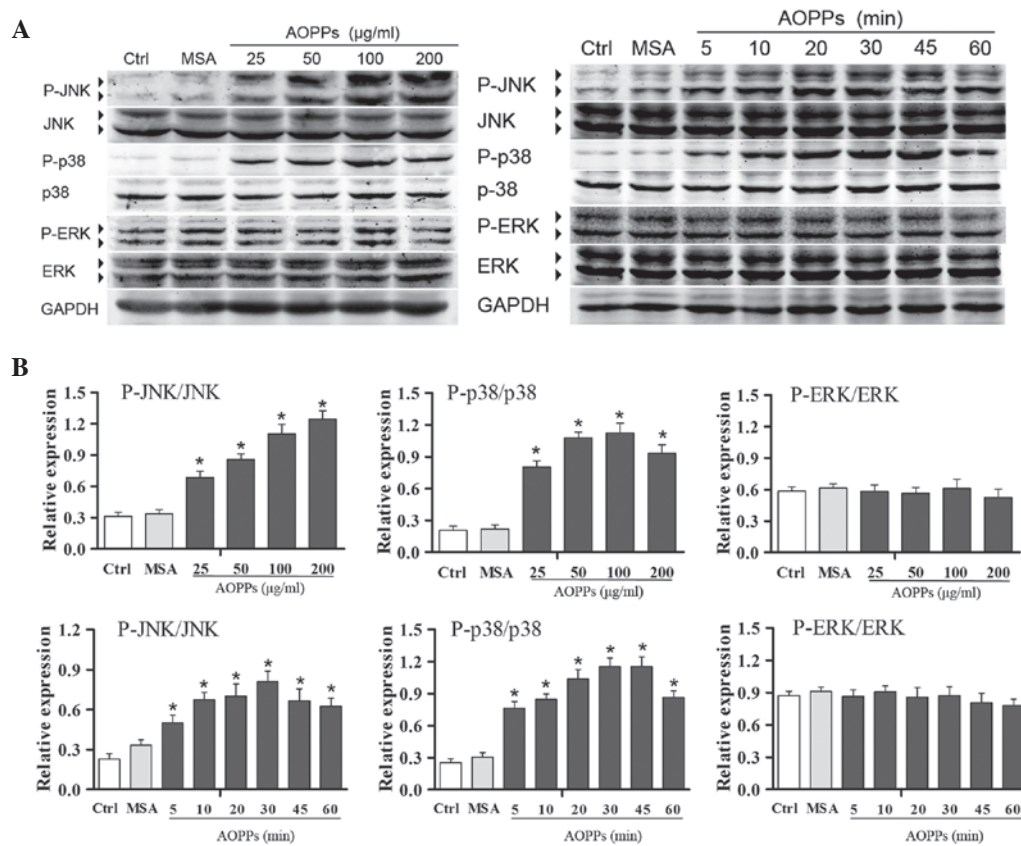


Figure 4. Treatment with advanced oxidation protein products (AOPPs) triggered activation of c-Jun N-terminal kinases (JNK) and p38 mitogen-activated protein kinases (MAPK) in MLO-Y4 cells. (A) Cells were treated with the indicated concentrations of AOPPs for 24 h, or with 200 µg/ml AOPPs for the indicated durations, prior to western blotting. (B) Blots were statistically analyzed. AOPPs induced activation of JNK and p38 MAPK in a dose- and time-dependent manner. Data are presented as the mean ± standard deviation of three independent experiments. Analysis of variance; *P<0.05 vs. control. Ctrl, control; MSA, mouse serum albumin; AOPPs, AOPPs-MSA; P-, phosphorylated; ERK, extracellular signal-regulated kinases; GAPDH, glyceraldehyde 3-phosphate dehydrogenase.

AOPPs induce ROS-dependent activation of JNK and p38 MAPK. The extent and duration of MAPK activation serves a key role in regulating cell functions (17,18). As shown in Fig. 4, activation of the JNK, p38 and ERK MAPKs was detected by western blotting, using phosphorylation level as an index of enzyme activity. Treatment of MLO-Y4 cells with AOPPs markedly induced the activation of JNK and p38, but not ERK, in a dose- and time-dependent manner. To further clarify the involvement of the activation of MAPKs in AOPPs-induced upregulation of sclerostin and RANKL, MLO-Y4 cells were pretreated with PD98059 (30 µM), SP600125 (30 µM) and SB203580 (30 µM) for 30 min, and were then co-treated with AOPPs (200 µg/ml) for the indicated durations. As shown in Fig. 5, SP600125 and SB203580, but not PD98059, significantly inhibited AOPPs-induced upregulation of sclerostin and RANKL, as confirmed by western blotting. These results indicate that AOPPs-induced upregulation of sclerostin and RANKL is associated with activation of JNK and p38 MAPK. As expected, NAC and apocynin effectively suppressed AOPPs-induced upregulation of sclerostin and RANKL (Fig. 5).

Discussion

AOPPs are known to induce apoptosis in several cell types (19-21); however, their effects on osteocytes remain

unclear. The present study demonstrated that AOPPs induced sustained activation of the JNK/p38 signaling pathways in a ROS-dependent manner, and consequently induced apoptosis of osteocytic MLO-Y4 cells. In addition, the results provided evidence to suggest that treatment of MLO-Y4 cells with AOPPs increased sclerostin and RANKL expression, and this upregulation was also associated with the JNK/p38 signaling pathways.

Osteocytes, which are the most abundant cell type in bones, are located deep within the mineralized matrix and communicate with each other and with other cells on the bone surface via cellular processes that are projected along the canaliculi (22,23). It has previously been reported that dysregulation of the osteocyte network is likely to increase bone fragility and account for the higher incidence of fractures in glucocorticoid-consuming patients (24). In the present study, treatment of MLO-Y4 cells with AOPPs induced significant apoptosis in a dose- and time-dependent manner. AOPPs were able to activate JNK and p38, but not ERK MAPK in MLO-Y4 cells. Proteins in the MAPK family are involved in various cellular responses, in particular, JNK and p38 are important mediators of apoptosis induced by stressful stimuli (25,26). Following pretreatment with the JNK and p38 specific inhibitors, SP600125 and SB203580, the present study successfully demonstrated that AOPPs-induced apoptosis of MLO-Y4 cells was markedly ameliorated. These

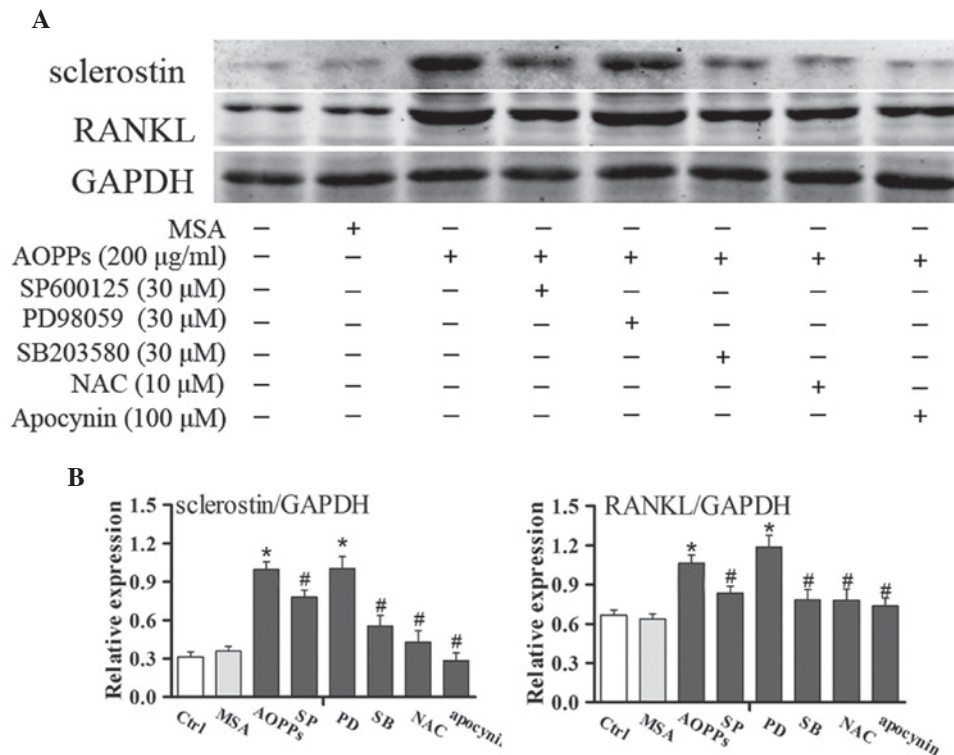


Figure 5. Effects of mitogen-activated protein kinases (MAPKs) signaling on advanced oxidation protein products (AOPPs)-induced upregulation of sclerostin and receptor activator of nuclear factor kappa-B ligand (RANKL) in MLO-Y4 cells. (A) Overnight serum-deprived MLO-Y4 cells were pretreated with SP600125, PD98059, SB203580, N-acetylcysteine (NAC) or apocynin for 30 min, and were then treated with 200 µg/ml AOPPs for 24 h. Sclerostin and RANKL expression were determined by western blotting. (B) Blots were statistically analyzed. Data are presented as the mean ± standard deviation of three independent experiments. Analysis of variance; *P<0.05 vs. control; #P<0.05 vs. AOPPs-treated group. Ctrl, untreated cells; MSA, mouse serum albumin; AOPPs, AOPPs-MSA; SP, SP600125; PD, PD98059; SB, SB203580; GAPDH, glyceraldehyde 3-phosphate dehydrogenase.

results indicated that JNK and p38 MAPK signaling are upstream pathways of AOPPs-induced apoptosis of MLO-Y4 cells. Notably, the present study also determined the effects of the NADPH oxidase inhibitor apocynin on AOPPs-induced apoptosis in MLO-Y4 cells. As expected, apocynin exerted an inhibitory effect on AOPPs-induced apoptosis in MLO-Y4 cells; however, the detailed signaling cascade involved was not under investigation in the present study.

ROS are known to serve critical roles in apoptosis (26-28), and in the present study, AOPPs were able to induce generation of a detectable level of intracellular ROS, as determined using the Cellular Reactive Species Detection Assay kit (Deep Red Fluorescence). Furthermore, it has previously been indicated that accumulated ROS induces sustained JNK and p38 MAPK activation, consequently leading to cell death (26). The results of the present study indicated that sustained phosphorylation of JNK and p38 MAPK was induced by ROS generation following AOPPs treatment. Notably, inhibition of ROS by NAC, a ROS scavenger, markedly abolished the effect of AOPPs on JNK and p38 MAPK activation, thus suggesting that AOPPs activate JNK and p38 MAPK signaling in a ROS-dependent manner.

Sclerostin and RANKL are two important proteins involved in bone remodeling. Encoded by the SOST gene, sclerostin is almost exclusively produced by osteocytes and binds to lipoprotein-receptor related protein (LRP-5) or -6 (LRP-6) domains. Sclerostin antagonizes LRP5/6-mediated canonical Wnt signaling within the osteoblast, thus inhibiting osteoblast

activity and promoting their apoptosis (29). Furthermore, sclerostin promotes osteoclast formation and activity via upregulation of RANKL production by osteocytes (30). In a previous study, overexpression of RANKL in transgenic mice led to severe cortical bone porosity, whereas an anti-RANKL antibody significantly improved cortical porosity in ovariectomized cynomolgus monkeys (31). The present study demonstrated that significant upregulation of sclerostin and RANKL expression was observed in AOPPs-challenged osteocytic MLO-Y4 cells. Furthermore, as determined following treatment with MAPK inhibitors, the AOPPs-induced upregulation of sclerostin and RANKL expression in MLO-Y4 cells was dependent on activation of the JNK/p38 MAPK signaling pathways.

There are some limitations to the present study. Firstly, the characteristics of the cultured osteocytic MLO-Y4 cells may not be identical to original osteocytes *in vivo*; therefore, further *in vivo* experiments are required to verify the present findings. In addition, it was not determined as to whether the AOPPs-induced production of sclerostin and RANKL was from the apoptotic MLO-Y4 cells or from the live cells.

In conclusion, the present study is the first, to the best of our knowledge, to demonstrate that AOPPs induced apoptosis of osteocytic MLO-Y4 cells via ROS-dependent JNK/p38 MAPK signaling. Furthermore, AOPPs stimulated the upregulation of sclerostin and RANKL in MLO-Y4 cells, which was also associated with activation of the JNK/p38 MAPK signaling pathways. These findings raise the possibility that AOPPs

contribute to the development of osteoporosis under certain medical conditions with excessive oxidative stress. Therefore, modulation of apoptotic pathways via the MAPK signaling cascade may be considered a therapeutic strategy for the prevention and treatment of secondary osteoporosis.

References

1. Witko-Sarsat V, Friedlander M, Capeillère-Blandin C, Nguyen-Khoa T, Zingraff J, Jungers P and Descamps-Latscha B: Advanced oxidation protein products as a novel marker of oxidative stress in uremia. *Kidney Int* 49: 1304-1313, 1996.
2. Witko-Sarsat V, Friedlander M, Nguyen Khoa T, Capeillère-Blandin C, Nguyen AT, Canteloup S, Dayer JM, Jungers P, Drüeke T and Descamps-Latscha B: Advanced oxidation protein products as novel mediators of inflammation and monocyte activation in chronic renal failure1, 2. *J Immunol* 161: 2524-2532, 1998.
3. Tucker PS, Dalbo VJ, Han T and Kingsley MI: Clinical and research markers of oxidative stress in chronic kidney disease. *Biomarkers* 18: 103-115, 2013.
4. Krzystek-Korpacka M, Neubauer K, Berdowska I, Boehm D, Zielinski B, Petryszyn P, Terlecki G, Paradowski L and Gamian A: Enhanced formation of advanced oxidation protein products in IBD. *Inflamm Bowel Dis* 14: 794-802, 2008.
5. Baskol G, Demir H, Baskol M, Kilic E, Ates F, Karakukcu C and Ustidal M: Investigation of protein oxidation and lipid peroxidation in patients with rheumatoid arthritis. *Cell Biochem Funct* 24: 307-311, 2006.
6. Piwowar A, Knapik-Kordecka M and Warwas M: AOPP and its relations with selected markers of oxidative/antioxidative system in type 2 diabetes mellitus. *Diabetes Res Clin Pract* 77: 188-192, 2007.
7. Painter SE, Kleerekoper M and Camacho PM: Secondary osteoporosis: A review of the recent evidence. *Endocr Pract* 12: 436-445, 2006.
8. Zhong ZM, Bai L and Chen JT: Advanced oxidation protein products inhibit proliferation and differentiation of rat osteoblast-like cells via NF-kappaB pathway. *Cell Physiol Biochem* 24: 105-114, 2009.
9. Sun N, Yang L, Li Y, Zhang H, Chen H, Liu D, Li Q and Cai D: Effect of advanced oxidation protein products on the proliferation and osteogenic differentiation of rat mesenchymal stem cells. *Int J Mol Med* 32: 485-491, 2013.
10. Yasuda H, Shima N, Nakagawa N, Yamaguchi K, Kinosaki M, Mochizuki S, Tomoyasu A, Yano K, Goto M, Murakami A, *et al*: Osteoclast differentiation factor is a ligand for osteoprotegerin/osteoclastogenesis-inhibitory factor and is identical to TRANCE/RANKL. *Proc Natl Acad Sci USA* 95: 3597-3602, 1998.
11. Nakashima T, Hayashi M, Fukunaga T, Kurata K, Oh-Hora M, Feng JQ, Bonewald LF, Kodama T, Wutz A, Wagner EF, *et al*: Evidence for osteocyte regulation of bone homeostasis through RANKL expression. *Nat Med* 17: 1231-1234, 2011.
12. Semenov M, Tamai K and Xi H: SOST is a ligand for LRP5/LRP6 and a wnt signaling inhibitor. *J Biol Chem* 280: 26770-26775, 2005.
13. Krause C, Korchynskiy O, de Rooij K, Weidauer SE, de Gorter DJ, van Bezooijen RL, Hatsell S, Economides AN, Mueller TD, Löwik CW and ten Dijke P: Distinct modes of inhibition by sclerostin on bone morphogenetic protein and Wnt signaling pathways. *J Biol Chem* 285: 41614-41626, 2010.
14. Kyriakis JM and Avruch J: Mammalian mitogen-activated protein kinase signal transduction pathways activated by stress and inflammation. *Physiol Rev* 81: 807-869, 2001.
15. Reddy KB, Nabha SM and Atanaskova N: Role of MAP kinase in tumor progression and invasion. *Cancer Metastasis Rev* 22: 395-403, 2003.
16. Livak KJ and Schmittgen TD: Analysis of relative gene expression data using real-time quantitative PCR and the 2- $\Delta\Delta$ CT method. *Methods* 25: 402-408, 2001.
17. Burotto M, Chiou VL, Lee JM and Kohn EC: The MAPK pathway across different malignancies: A new perspective. *Cancer* 120: 3446-3456, 2014.
18. Thouverey C and Caverzasio J: Focus on the p38 MAPK signaling pathway in bone development and maintenance. *Bonekey Rep* 4: 711, 2015.
19. Wang SS, Huang QT, Zhong M and Yin Q: AOPPs (advanced oxidation protein products) promote apoptosis in trophoblastic cells through interference with NADPH oxidase signaling: Implications for preeclampsia. *J Matern Fetal Neonatal Med* 28: 1747-1755, 2015.
20. Zhou LL, Cao W, Xie C, Tian J, Zhou Z, Zhou Q, Zhu P, Li A, Liu Y, Miyata T, *et al*: The receptor of advanced glycation end products plays a central role in advanced oxidation protein products-induced podocyte apoptosis. *Kidney Int* 82: 759-770, 2012.
21. Xie F, Sun S, Xu A, Zheng S, Xue M, Wu P, Zeng JH and Bai L: Advanced oxidation protein products induce intestine epithelial cell death through a redox-dependent, c-jun N-terminal kinase and poly (ADP-ribose) polymerase-1-mediated pathway. *Cell Death Dis* 5: e1006, 2014.
22. Bonewald LF: The amazing osteocyte. *J Bone Res* 26: 229-238, 2011.
23. Compton JT and Lee FY: A review of osteocyte function and the emerging importance of sclerostin. *J Bone Joint Surg Am* 96: 1659-1668, 2014.
24. Seibel MJ, Cooper MS and Zhou H: Glucocorticoid-induced osteoporosis: Mechanisms, management and future perspectives. *Lancet Diabetes Endocrinol* 1: 59-70, 2013.
25. Osone S, Hosoi H, Kuwahara Y, Matsumoto Y, Iehara T and Sugimoto T: Fenretinide induces sustained-activation of JNK/p38 MAPK and apoptosis in a reactive oxygen species-dependent manner in neuroblastoma cells. *Int J Cancer* 112: 219-224, 2004.
26. Park GB, Choi Y, Kim YS, Lee HK, Kim D and Hur DY: ROS-mediated JNK/p38-MAPK activation regulates bax translocation in sorafenib-induced apoptosis of EBV-transformed B cells. *Int J Oncol* 44: 977-985, 2014.
27. Lee SY, Kang SU, Kim KI, Kang S, Shin YS, Chang JW, Yang SS, Lee K, Lee JS, Moon E and Kim CH: Nonthermal plasma induces apoptosis in ATC cells: Involvement of JNK and p38 MAPK-dependent ROS. *Yonsei Med J* 55: 1640-1647, 2014.
28. Palit S, Kar S, Sharma G and Das PK: Hesperetin induces apoptosis in breast carcinoma by triggering accumulation of Ros and activation of ASK1/JNK Pathway. *J Cell Physiol* 230: 1729-1739, 2015.
29. Winkler DG, Sutherland MK, Geoghegan JC, Yu C, Hayes T, Skonier JE, Shpektor D, Jonas M, Kovacevich BR, Staehling-Hampton K, *et al*: Osteocyte control of bone formation via sclerostin, a novel BMP antagonist. *EMBO J* 22: 6267-6276, 2003.
30. Wijenayaka AR, Kogawa M, Lim HP, Bonewald LF, Findlay DM and Atkins GJ: Sclerostin stimulates osteocyte support of osteoclast activity by a RANKL-dependent pathway. *PLoS one* 6: e25900, 2011.
31. Kostenuik PJ, Smith SY, Jolette J, Schroeder J, Pyrah I and Ominsky MS: Decreased bone remodeling and porosity are associated with improved bone strength in ovariectomized cynomolgus monkeys treated with denosumab, a fully human RANKL antibody. *Bone* 49: 151-161, 2011.